nature structural & molecular biology

Human RECQ1 promotes restart of replication forks reversed by DNA topoisomerase I inhibition

Matteo Berti[1,11], Arnab Ray Chaudhuri[2,11], Saravanabhavan Thangavel[1], Shivasankari Gomathinayagam[1], Sasa Kenig[3], Marko Vujanovic[2], Federico Odreman[4], Timo Glatter[5,10], Simona Graziano[1], Ramiro Mendoza-Maldonado[4], Francesca Marino[3], Bojana Lucic[4], Valentina Biasin[4], Matthias Gstaiger[5,6], Ruedi Aebersold[5–7], Julia M Sidorova[8], Raymond J Monnat Jr[8,9], Massimo Lopes[2] & Alessandro Vindigni[1]

Topoisomerase I (TOP1) inhibitors are an important class of anticancer drugs. The cytotoxicity of TOP1 inhibitors can be modulated by replication fork reversal through a process that requires poly(ADP-ribose) polymerase (PARP) activity. Whether regressed forks can efficiently restart and what factors are required to restart fork progression after fork reversal are still unknown. We have combined biochemical and EM approaches with single-molecule DNA fiber analysis to identify a key role for human RECQ1 helicase in replication fork restart after TOP1 inhibition that is not shared by other human RecQ proteins. We show that the poly(ADP-ribosyl)ation activity of PARP1 stabilizes forks in the regressed state by limiting their restart by RECQ1. These studies provide new mechanistic insights into the roles of RECQ1 and PARP in DNA replication and offer molecular perspectives to potentiate chemotherapeutic regimens based on TOP1 inhibition.

TOP1 inhibitors are an important class of anticancer drugs that exert their function by perturbing DNA replication[1,2]. The mechanisms of tumor response to TOP1 inhibitors and combinations of TOP1 inhibitors with other drugs for more effective tumor treatment are areas of active investigation[3,4]. One widely accepted mechanism for the cytotoxicity of TOP1 inhibitors has been their ability to create single-strand breaks (SSBs), which are converted to toxic DNA double-strand breaks (DSBs) upon colliding with the replication fork during replication[5]. This notion was recently challenged by the discovery that TOP1 inhibitors also impair TOP1 relaxation activity, inducing an accumulation of positive supercoils ahead of the replication fork that may hamper fork progression and the conversion of SSBs to DSBs[1,6]. Recent studies extended this observation by showing that replication forks rapidly slow and undergo fork reversal upon treatment with clinically relevant doses of camptothecin (CPT), the prototype TOP1 inhibitor[7,8]. This prevents DSB formation and requires the activity of PARP1, a well-known chromatin-associated enzyme that modifies various nuclear proteins by poly(ADP-ribosyl)ation (PARylation), to accumulate regressed forks[7]. However, the exact role of PARP1 in promoting fork reversal remains unexplained. In addition, other factors are likely to be involved in this process, and the protein(s) required to restore and restart reversed replication forks after the lesion is repaired have not been identified.

RecQ helicases have long been proposed to assist replication forks in dealing with replication stress and have attracted considerable interest in recent years owing to their connection to heritable human diseases associated with cancer predisposition[9,10]. RecQ helicase enzymatic activities (such as DNA unwinding, branch migration and strand annealing) may have multiple roles during replication by virtue of their ability to interconvert numerous replication and recombination intermediates[11–13]. Moreover, previous studies have pointed to a potential role of RecQ helicases in fork reversal and restart by showing that two of the five human RecQ helicases, BLM and WRN, promote both regression and re-establishment of model replication forks *in vitro*[14–16]. However, distinct roles or molecular functions for the five human RecQ helicases in replication stress and cancer remain to be defined[10,17].

For the present study, we combined biochemical, single-molecule DNA fiber and EM approaches to investigate the function of the human RECQ1 helicase (also known as RECQL or RECQL1) during the replication stress response. Of the five human RecQ proteins, RECQ1 was the first to be discovered, owing to its potent ATPase activity, and it is the most abundant in cells[18,19]. However, little is known about its cellular functions to date. Here, we show that RECQ1 has an essential role—one not shared by other human RecQ helicases—in restoring active replication forks that have regressed as a result of TOP1 inhibition. Moreover, we provide a rationale for the

[1]Department of Biochemistry and Molecular Biology, Saint Louis University School of Medicine, St. Louis, Missouri, USA. [2]Institute of Molecular Cancer Research, University of Zurich, Zurich, Switzerland. [3]Structural Biology Laboratory, Sincrotrone Trieste, Trieste, Italy. [4]International Centre for Genetic Engineering and Biotechnology, Trieste, Italy. [5]Institute for Molecular Systems Biology, Swiss Federal Institute of Technology (ETH) Zurich, Zurich, Switzerland. [6]Competence Center for Systems Physiology and Metabolic Diseases, ETH Zurich, Zurich, Switzerland. [7]Faculty of Science, University of Zurich, Zurich, Switzerland. [8]Department of Pathology, University of Washington, Seattle, Washington, USA. [9]Department of Genome Sciences, University of Washington, Seattle, Washington, USA. [10]Present address: Proteomics Core Facility, Biozentrum, University of Basel, Basel, Switzerland. [11]These authors contributed equally to this work. Correspondence should be addressed to A.V. (avindign@slu.edu) or M.L. (lopes@imcr.uzh.ch).

Received 18 June 2012; accepted 26 December 2012; published online 10 February 2013; doi:10.1038/nsmb.2501

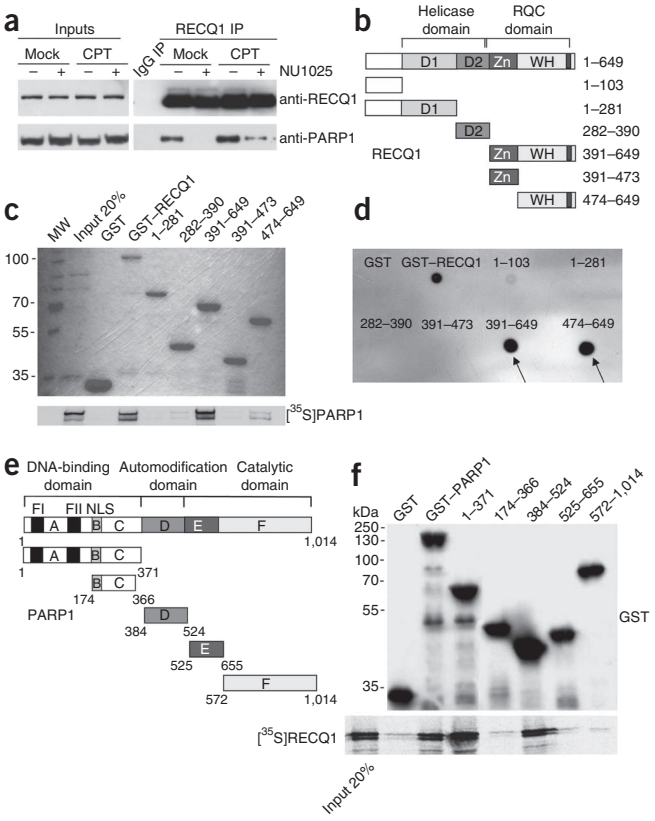

Figure 1 Analysis of the RECQ1-PARP1 interaction. (**a**) Immunoprecipitation from U-2 OS cells using the anti-RECQ1 antibody with (+) or without (–) NU1025 (50 μM) and with CPT (100 nM for 2 h) or without DNA damage (mock). Rabbit IgG IP served as a negative control. Immunoblots were developed with anti-RECQ1 and anti-PARP1 antibodies. (**b**) Schematic representation of the domain structure of RECQ1 and the GST-tagged RECQ1 fragments. D1 and D2, RecA-like domains. (**c**) Pulldown assays with GST-tagged RECQ1 fragments. Top, Coomassie-stained gel of GST-RECQ1 fragments. Bottom, autoradiography of *in vitro* GST pulldown assay using ^{35}S-labeled PARP1. MW, molecular weight (kDa). (**d**) Analysis of PAR binding to GST-RECQ1 fragments (2 pmol) dot-blotted onto a nitrocellulose membrane. The arrows indicate the two RECQ1 fragments that interact with ^{32}P-labeled PAR. (**e**) Schematic representation of the domain structure of PARP1 and the GST-tagged PARP1 fragments: A, DNA binding domain; B, nuclear localization signal; D, BRCT automodification domain; E, contains a WGR motif; F, catalytic domain; FI and FII, zinc-finger motifs; NLS, nuclear localization sequence. A third zinc-finger motif has been recently identified in domain C[36,37] in addition to FI and FII. (**f**) Pulldown assays with GST-tagged PARP1 (GST-PARP) fragments. Bound proteins were detected by autoradiography (bottom). Purified GST or GST-PARP1 proteins were detected with an anti-GST antibody (top). Input, 20% of the amount used in binding reactions.

requirement of the PARylation activity of PARP1 in replication fork reversal. Our observations give new insight into a pivotal mechanism responsible for replication stress response and replication fork restart after chemotherapeutic drug damage. These findings have important clinical implications, as RECQ1 inactivation might affect the efficacy of combinatorial therapies that employ PARP inhibitors and DNA-damaging agents and are already in promising clinical trials.

RESULTS

RECQ1 interacts with PARP1 and PAR

To better define the role of human RECQ1 helicase in DNA replication and repair, we first identified proteins associated with RECQ1 using a new, integrated proteomic approach[20]. We used human embryonic kidney (HEK293) cells to generate a stable, inducible cell line expressing a doubly tagged version of RECQ1 (consisting of a streptavidin-binding peptide and a hemagglutinin epitope tag), then isolated protein complexes containing RECQ1 by affinity purification (**Supplementary Fig. 1a–d**); we characterized the resulting complexes by MS[20]. Among the most abundant co-purified proteins were PARP1, Ku70 and Ku80 (key components of the DNA nonhomologous end–joining pathway) and several nucleosomal components (**Supplementary Fig. 1e**). Given recent reports indicating a role for PARP1 in replication stress response[7,21], we decided to focus our work on defining the role of RECQ1 interactions with PARP1.

We confirmed the RECQ1-PARP1 interaction by co-immunoprecipitation (co-IP) using nuclear extracts from human osteosarcoma (U-2 OS) cells and an antibody to RECQ1 (anti-RECQ1) that recognizes the C terminus of RECQ1 (residues 633–648). We obtained similar results using an anti-RECQ1 antibody that recognizes the N terminus of the protein (data not shown). We also performed reciprocal co-IPs using an anti-PARP1 antibody (**Fig. 1a** and **Supplementary Fig. 1f**). All co-IPs were performed in the presence of ethidium bromide or Benzonase to ensure that DNA did not mediate the interactions. We obtained similar results with other cell lines (**Supplementary Fig. 1f** and data not shown), indicating that the association between RECQ1 and PARP1 is not cell-type specific. These observations are in agreement with a previous report showing that RECQ1 and PARP1 interact at viral replication origins and with a recent study reporting an interaction between RECQ1 and PARP1 in human cells[22,23].

The RECQ1–PARP1 interaction is regulated by PARP1 PARylation activity: we observed increased association of the two proteins upon DNA damage and sharply reduced association upon inhibition of PARP1 activity with the PARP inhibitor NU1025 (**Fig. 1a** and **Supplementary Fig. 1g**). Using recombinant, purified PARP1 and RECQ1, we found that these two proteins interact directly, and the interaction was considerably stronger when we used a PARylated form of PARP1, indicating that the PAR modification of PARP1 is important for the interaction with RECQ1 (**Supplementary Fig. 2a**,**b**). Indeed, we observed that RECQ1 interacted with PAR, and binding to PAR was resistant to extensive washing with 1 M salt, although we could not identify any canonical PAR binding motifs in RECQ1 (ref. 24) (**Supplementary Fig. 2c**). We verified that NU1025 did not affect the interaction between recombinant RECQ1 and PARP1 *in vitro*, indicating that the reduced RECQ1-PARP1 interaction we observed by co-IP in the presence of this inhibitor is due to the inhibition of PARP1 PARylation activity rather than to a potential effect of NU1025 on PARP conformation (**Supplementary Fig. 2b**).

We next mapped the domains of RECQ1 that interact with PARP1 and PAR using a series of glutathione *S*-transferase (GST)-tagged RECQ1 fragments (**Fig. 1b–d**). Both PARP1 and PAR interacted with the C-terminal region of RECQ1 (residues 391–649; fragment names below indicate residue numbers), which contains the zinc-binding (Zn) and winged helix (WH) domains that form the 'RecQ–C-terminal' (RQC) domain, but not with fragment 391–473, which contains the Zn domain alone (**Fig. 1c**). The WH domain alone (fragment 474–649) also bound PARP1, although more weakly than fragment 391–649. These results suggest that the region containing residues 391–473 might be important for the stability and/or conformation of the WH domain. Our data also suggest that the region containing residues 391–649 is PARylated by PARP1 *in vitro* (**Supplementary Fig. 2d** and **Supplementary Note**); however, RECQ1 does not seem to be PARylated *in vivo*[22].

To determine which region(s) of PARP1 are involved in RECQ1 interaction, we overexpressed truncated versions of PARP1 fused to

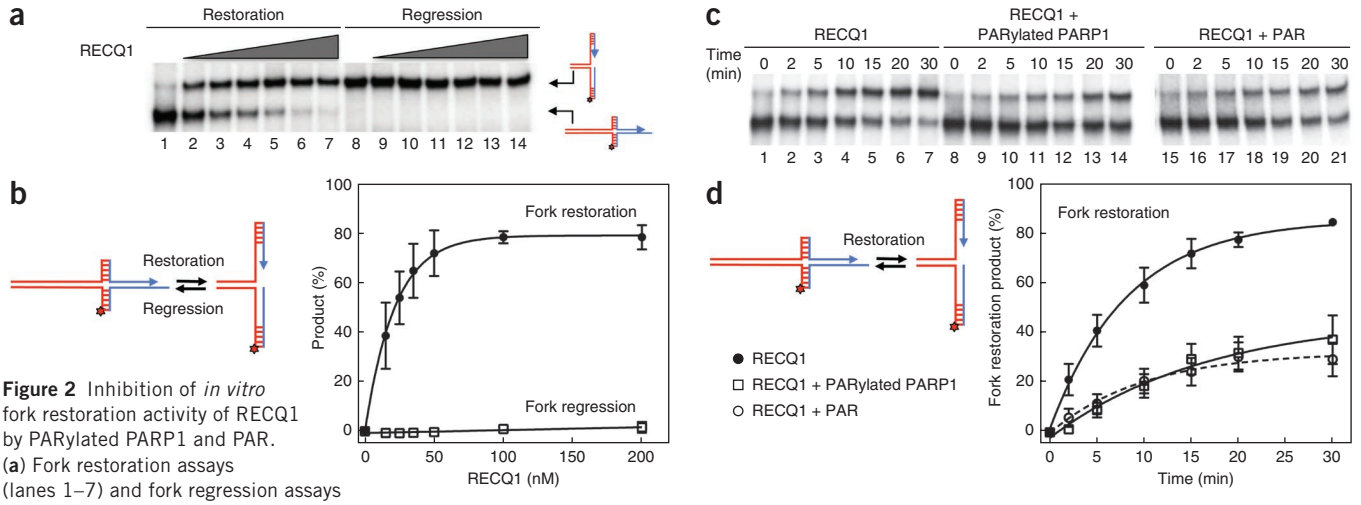

Figure 2 Inhibition of *in vitro* fork restoration activity of RECQ1 by PARylated PARP1 and PAR. (**a**) Fork restoration assays (lanes 1–7) and fork regression assays (lanes 8–14) performed using increasing RECQ1 concentrations (0, 15, 25, 35, 50, 100 and 200 nM) and a fixed concentration of chicken-foot substrate (2 nM, for restoration assay) or replication fork structure (2 nM, for regression assay). Right, schematic of the reaction products. (**b**) Left, schematic of restoration and regression reactions. Lined regions indicate heterologous sequences included in the vertical arms to prevent complete strand separation. In addition, we inserted two mismatches and a single isocytosine modification to prevent spontaneous fork regression and restoration (**Supplementary Fig. 3**). Stars indicate [γ-^{32}P]ATP-labeled 5 ends. Right, percentage of fork restoration and regression products plotted as a function of protein concentration. (**c**) Kinetic experiments using RECQ1 (40 nM) and the chicken-foot substrate (2 nM), visualized by gel electrophoresis. Lanes 1–7, RECQ1 alone; lanes 8–14, RECQ1 in the presence of PARylated PARP1 (40 nM); lanes 15–21, RECQ1 in the presence of PAR (100 nM). (**d**) Left, schematic of restoration reaction. Right, percentage of fork restoration for RECQ1 alone and RECQ1 in the presence of PARylated PARP1 or PAR. Data in **a**–**d** represent the mean of three independent experiments. Error bars, s.e.m.

GST in HeLa cells (**Fig. 1e**,**f**). Only fragments 1–371 and 384–524 could efficiently pull down RECQ1 in immunoprecipitation experiments, and fragment 174–366 did not pull down RECQ1. These results indicate that the interaction with RECQ1 involves the first 173 N-terminal residues of PARP1 (containing the DNA binding domain) and residues 384–524 (containing the BRCT domain, which is also the automodification domain). These two PARP1 domains are also involved in homodimerization and the binding of several partners, including WRN helicase[25,26].

RECQ1 catalyzes restoration of synthetic replication forks

On the basis of the recent discovery that PARP1 has an important role in reversal of replication forks after CPT treatment[7], we investigated whether RECQ1 is required for the cellular response to TOP1 inhibition. First, we confirmed previous observations that RECQ1 depletion leads to increased CPT sensitivity[27]. Flow-cytometric analysis showed that RECQ1-depleted cells are only mildly sensitive to most replication inhibitors and DNA-damaging agents, apart from CPT and etoposide (**Supplementary Fig. 3a** and **Supplementary Note**). These two drugs inhibit DNA replication by suppressing the relaxation activity of the type IB and type IIA topoisomerases, respectively[2]. Next, to confirm that RECQ1 binds to replication forks *in vivo* and that the interaction increases upon CPT treatment, we labeled newly replicated DNA with 5-chlorodeoxyuridine (CldU), and confirmed RECQ1 co-IP with CldU in the presence and absence of CPT (**Supplementary Fig. 3b** and **Supplementary Note**).

We then tested whether RECQ1 mediates replication fork regression and/or restoration on synthetic DNA substrates and whether PARP1 affects RECQ1 activity. To measure these RECQ1 activities *in vitro*, we used a set of four oligonucleotides that can anneal into two alternative substrates that mimic model replication fork and 'chicken-foot' structures[14,28] (**Supplementary Fig. 3c** and **Supplementary Table 1**). We found that RECQ1 promotes model replication fork restoration very efficiently and in a concentration-dependent fashion: 50 nM RECQ1 converted >75% of the chicken-foot structure into the model replication fork after 20 min (**Fig. 2a**,**b**). In contrast, RECQ1 failed to catalyze the opposite reaction (fork regression): we detected <2% of chicken-foot structure, even at the highest RECQ1 concentration. We obtained identical results using a variant of the same substrate lacking the 6-nucleotide (nt) single-stranded DNA (ssDNA) gap on the leading-strand template, thus ruling out the possibility that the presence of the ssDNA gap prevented RECQ1-mediated fork regression (**Supplementary Figs. 3d** and **4a**). Next, we confirmed that the ATPase activity of RECQ1 is essential to promote branch migration of the chicken-foot structure and restoration of the active replication fork. We observed that the poorly hydrolyzable ATP analog ATPγS and the nonhydrolyzable analog AMP-PNP strongly inhibited the reaction, and two previously characterized ATPase-deficient RECQ1 mutants, K119R and E220Q, lacked fork restoration (**Supplementary Fig. 4b**). Additional experiments using Holliday junction substrates with heterology regions of 1 and 4 bases confirmed that RECQ1 has a strong branch migration activity and that its helicase activity may be important to bypass regions of heterology. However, we observed a 50% reduction in the formation of the branch migration product when the heterology region was increased from 1 to 4 bases (**Supplementary Fig. 5a**,**b**).

On the basis of our results showing that RECQ1 interacts with PARylated PARP1 and previous observations that the PARylation activity of PARP has a key role in mediating the accumulation of regressed forks after DNA damage[7], we examined the effect of PARylated PARP1 on RECQ1 fork restoration activity. We found that PARylated PARP1 strongly inhibited the fork restoration rates of RECQ1: 40 nM RECQ1 converted approximately 80% of the chicken-foot structure into a replication fork structure within 20 min. Addition of an equimolar concentration of PARylated PARP1 reduced the fraction of restored fork structures to <30% (**Fig. 2c**,**d**). Experiments performed at increasing concentrations of PARylated PARP1 showed that a two-fold excess of PARylated PARP1 did not inhibit the reaction further, indicating that equimolar concentrations are sufficient for maximal inhibition (**Supplementary Fig. 4c**). We observed a similar

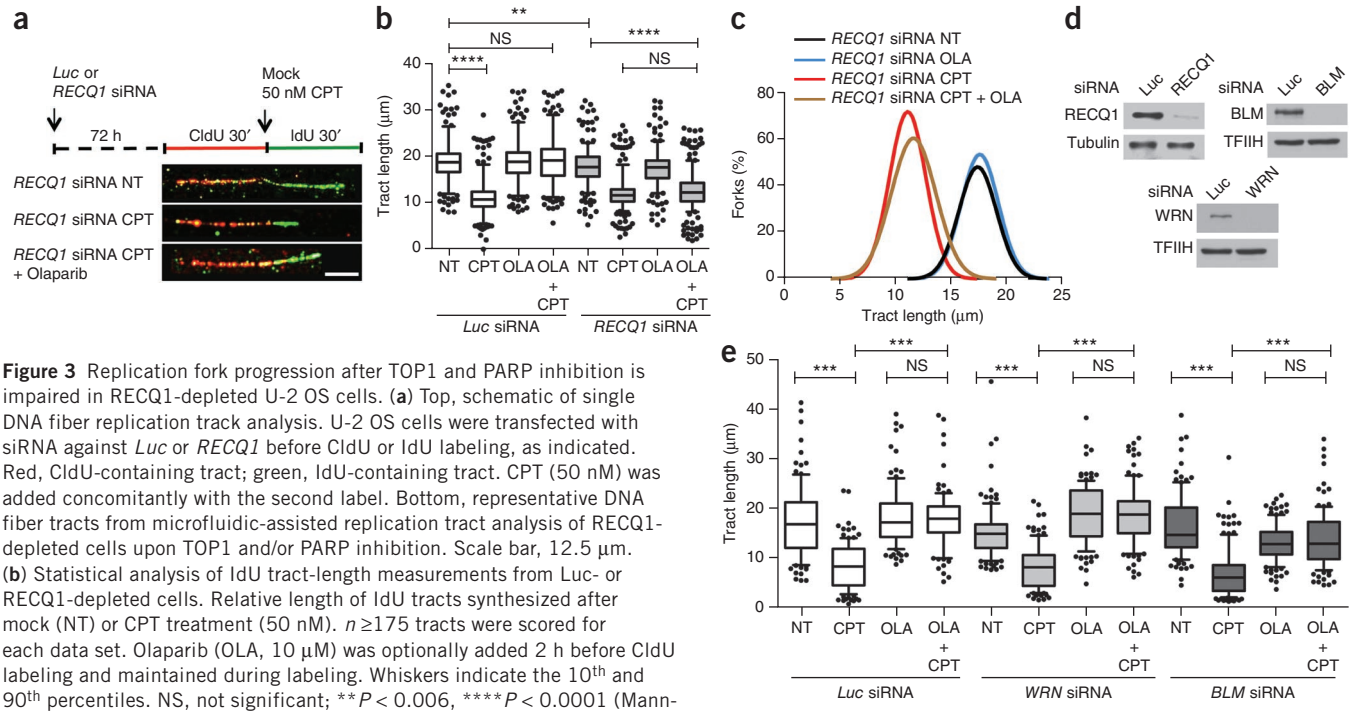

Figure 3 Replication fork progression after TOP1 and PARP inhibition is impaired in RECQ1-depleted U-2 OS cells. (**a**) Top, schematic of single DNA fiber replication track analysis. U-2 OS cells were transfected with siRNA against *Luc* or *RECQ1* before CldU or IdU labeling, as indicated. Red, CldU-containing tract; green, IdU-containing tract. CPT (50 nM) was added concomitantly with the second label. Bottom, representative DNA fiber tracts from microfluidic-assisted replication tract analysis of RECQ1-depleted cells upon TOP1 and/or PARP inhibition. Scale bar, 12.5 μm. (**b**) Statistical analysis of IdU tract-length measurements from Luc- or RECQ1-depleted cells. Relative length of IdU tracts synthesized after mock (NT) or CPT treatment (50 nM). $n \geq 175$ tracts were scored for each data set. Olaparib (OLA, 10 μM) was optionally added 2 h before CldU labeling and maintained during labeling. Whiskers indicate the 10th and 90th percentiles. NS, not significant; $^{**}P < 0.006$, $^{****}P < 0.0001$ (Mann-Whitney test). (**c**) Smoothed histogram of IdU tract-length distribution after TOP1 and/or PARP inhibition in RECQ1-depleted (*RECQ1* siRNA) cells. (**d**) RECQ1, BLM and WRN expression after siRNA knockdown, detected by western blotting. Tubulin and transcription factor II H (TFIIH) were detected as loading controls. (**e**) Statistical analysis of IdU tract-length measurements from Luc-, WRN- and BLM-depleted cells, as in **b**. $^{***}P < 0.0001$.

inhibition of RECQ1 activity in the presence of PARylated PARP1 using the Holliday junction (**Supplementary Fig. 5c,d**). To confirm that PARylated PARP1 is also able to inhibit the DNA unwinding activity of RECQ1, we used a fork duplex substrate with a duplex region of 20 bp (**Supplementary Fig. 5e,f**). In agreement with previous findings[29], electrophoretic mobility shift assays using increasing concentrations of PARylated PARP1 confirmed that PARylated PARP1 binds DNA with low affinity, indicating that the inhibitory effect of PARylated PARP1 on RECQ1 activity is not due to a competition for DNA binding (**Supplementary Fig. 6**). Additional fork restoration assays performed with PAR instead of PARylated PARP1 supported this conclusion, confirming that the interaction of RECQ1 with PAR is responsible for the inhibition of the fork restoration activity (**Fig. 2**). Collectively, our biochemical data show that RECQ1 has strong fork restoration activity that could be responsible for restarting reversed forks associated with CPT treatment. PARylated PARP1 inhibits this RECQ1 activity through a process that does not involve competition for DNA binding.

To investigate whether other human RecQ helicases share this activity, we performed additional experiments with an exonuclease-deficient WRN mutant (WRN-E84A) that allows the branch migration reaction to be monitored without possible complications arising from substrate digestion. WRN-E84A promoted fork restoration and regression with similar efficiency, with a slight bias toward fork restoration (**Supplementary Fig. 7**). Furthermore, the presence of PARylated PARP1 did not inhibit the fork restoration activity of WRN-E84A, in agreement with previous studies in which a different set of substrates was used[26]. These results, along with previous observations for BLM[14], show that although other helicases are able to promote fork restoration and regression, RECQ1 has a marked preference to promote fork restoration over fork regression, and its activity is uniquely regulated by PARylated PARP1.

RECQ1 and PARP control CPT-induced replication fork slowing

Next, we used genome-wide single-molecule DNA replication assays to test whether RECQ1 depletion affects the rate of replication fork progression upon TOP1 inhibition in a cellular context. We pulse-labeled U-2 OS cells with the thymidine analog CIdU for 30 min then treated cells with 50 nM CPT, concomitantly labeling them with a second thymidine analog (IdU) for an additional 30 min (**Fig. 3**). We then analyzed the IdU tract-length distributions after CPT treatment with or without PARP inhibition. Using this approach, we initially confirmed previous findings that replication forks rapidly slow upon treatment with low CPT doses (50 nM), and that this effect requires the action of PARP1 (refs. 7,8). This is consistent with the notion that PARP inactivation does not perturb normal fork progression but prevents fork slowing after TOP1 inhibition. We then measured rates of fork progression in RECQ1-depleted cells treated with CPT and the PARP inhibitor olaparib. Our results showed that PARP inhibition does not rescue CPT-induced fork slowing in RECQ1-deficient cells. These results identify an essential role for RECQ1 in the control of fork progression upon TOP1 inhibition. RECQ1 downregulation using a lentiviral system and a different RNA interference (RNAi) targeting sequence showed similar results, supporting the notion that the observed effect was specifically associated with RECQ1 loss (**Fig. 4** and data not shown). Additional DNA fiber experiments showed that—in contrast to the results obtained with RECQ1-depleted cells—PARP inhibition was still able to rescue CPT-induced fork slowing in BLM- and WRN-depleted cells. These results strongly support the notion that the identified role of RECQ1 in the control of fork progression upon TOP1 inhibition reflects a specific function and not a more general role of the RecQ helicase family (**Fig. 3e**). Genetic knockdown–rescue experiments confirmed that complementation in RECQ1-depleted U-2 OS cells with short hairpin RNA (shRNA)-resistant wild-type RECQ1 abrogated the effect of RECQ1

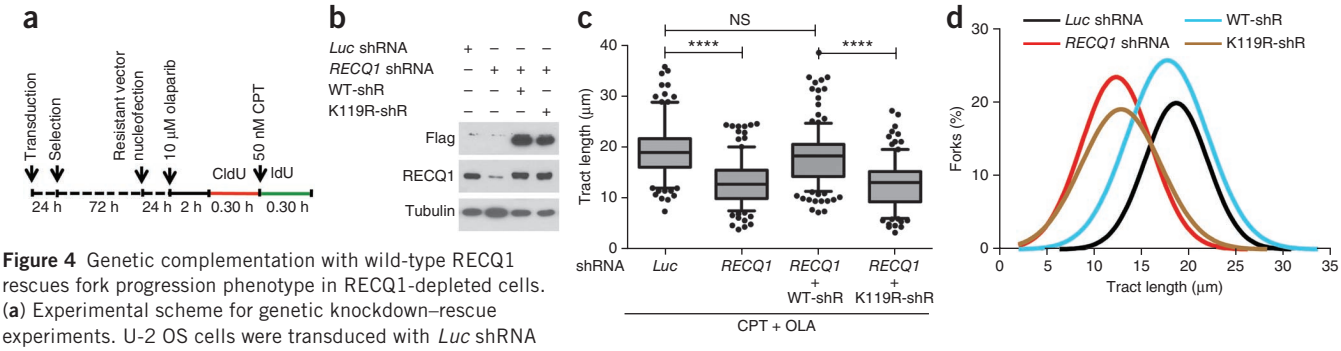

Figure 4 Genetic complementation with wild-type RECQ1 rescues fork progression phenotype in RECQ1-depleted cells. (**a**) Experimental scheme for genetic knockdown–rescue experiments. U-2 OS cells were transduced with *Luc* shRNA or *RECQ1* shRNA. RECQ1-depleted cells were nucleofected to express RNAi-resistant wild-type (WT-shR) or K119R (K119R-shR) RECQ1 before CldU labeling. (**b**) Western blot analysis of RECQ1-depleted cells expressing Flag-tagged WT-shR or K119R-shR. Tubulin was detected as a loading control. (**c**) Statistical analysis of IdU tract-length measurements from **a**. Relative length of IdU tracts synthesized after CPT treatment (50 nM). $n \geq 175$ tracts were scored for each data set. Olaparib (10 μM) was added 2 h before CldU labeling and maintained during labeling. Whiskers indicate the 10th and 90th percentiles. NS, not significant; $^{****}P < 0.0001$ (Mann-Whitney test). (**d**) Smoothed histogram of IdU tract length after TOP1 and PARP inhibition in RECQ1-depleted cells alone and genetically complemented with WT-shR or K119R-shR.

depletion on replication fork progression upon TOP1 inhibition (**Fig. 4**). Moreover, expression of the ATPase-deficient RECQ1 mutant K119R in RECQ1-depleted cells confirmed that the ATPase activity of RECQ1 is essential for its role in replication fork progression upon TOP1 inhibition (**Fig. 4**). Notably, we observed a minor but statistically significant ($P < 0.006$) difference between the mean length of the replication tracts measured in RECQ1-depleted cells relative to luciferase-depleted cells in the absence of CPT treatment (**Fig. 3b**). This is in line with our previous studies, in which we observed that the replication tracts were slightly shorter in RECQ1-depleted cells than in luciferase-depleted control cells in the absence of DNA damage[19]. These data might reflect an additional role for RECQ1 in replication fork progression in unperturbed cells.

Previous work has showed that CPT-induced fork slowing is uncoupled from DSB formation in human cells[7]. To determine whether RECQ1 depletion also influenced DSB accumulation after CPT treatment, we used a recently optimized pulsed-field gel electrophoresis (PFGE) protocol[7,30]. Our PFGE analysis confirmed that PARP inhibition in U-2 OS cells leads to the induction of high levels of DSBs after CPT treatment (100 nM) (**Fig. 5a**,**b**). These results are consistent with the notion that PARP-inhibited or PARP-depleted cells do not slow or accumulate reversed forks after CPT treatment, leading to DSB formation even at low CPT doses[7]. RECQ1 depletion, however, had the opposite effect: PARP1 inhibition did not prevent fork slowing after CPT or lead to increased DSB formation in RECQ1-depleted cells (**Fig. 5a**,**b**). As an alternative method of monitoring DSB formation, we looked at phosphorylated histone H2AX (γH2AX) and p53-binding protein 1 (53BP1) foci colocalization under the same conditions used for the PFGE experiments. In agreement with previous findings, we found that only a minor fraction of γH2AX foci colocalized with 53BP1 upon 100 nM CPT treatment and that PARP inhibition led to a considerably higher degree of γH2AX and 53BP1 colocalization[7] (**Fig. 5c**,**d**). However, RECQ1 depletion reduced the fraction of colocalizing foci in the presence of olaparib, supporting

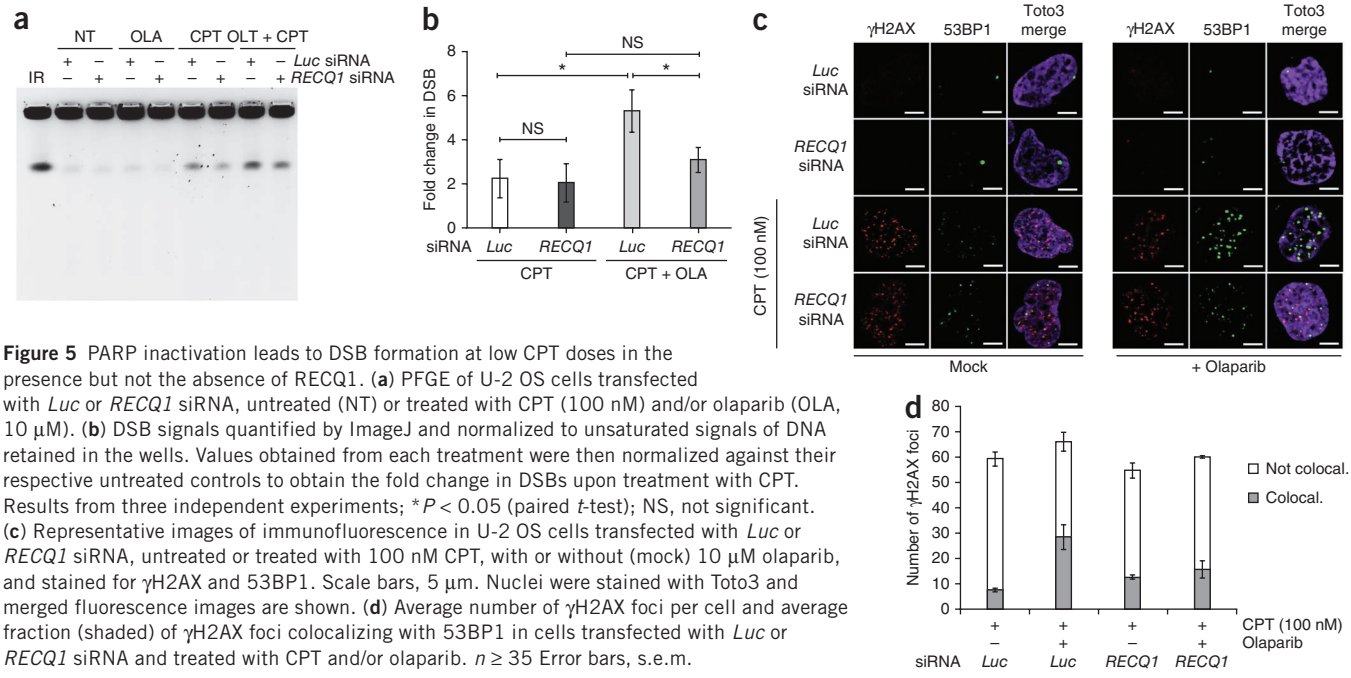

Figure 5 PARP inactivation leads to DSB formation at low CPT doses in the presence but not the absence of RECQ1. (**a**) PFGE of U-2 OS cells transfected with *Luc* or *RECQ1* siRNA, untreated (NT) or treated with CPT (100 nM) and/or olaparib (OLA, 10 μM). (**b**) DSB signals quantified by ImageJ and normalized to unsaturated signals of DNA retained in the wells. Values obtained from each treatment were then normalized against their respective untreated controls to obtain the fold change in DSBs upon treatment with CPT. Results from three independent experiments; $^{*}P < 0.05$ (paired *t*-test); NS, not significant. (**c**) Representative images of immunofluorescence in U-2 OS cells transfected with *Luc* or *RECQ1* siRNA, untreated or treated with 100 nM CPT, with or without (mock) 10 μM olaparib, and stained for γH2AX and 53BP1. Scale bars, 5 μm. Nuclei were stained with Toto3 and merged fluorescence images are shown. (**d**) Average number of γH2AX foci per cell and average fraction (shaded) of γH2AX foci colocalizing with 53BP1 in cells transfected with *Luc* or *RECQ1* siRNA and treated with CPT and/or olaparib. $n \geq 35$ Error bars, s.e.m.

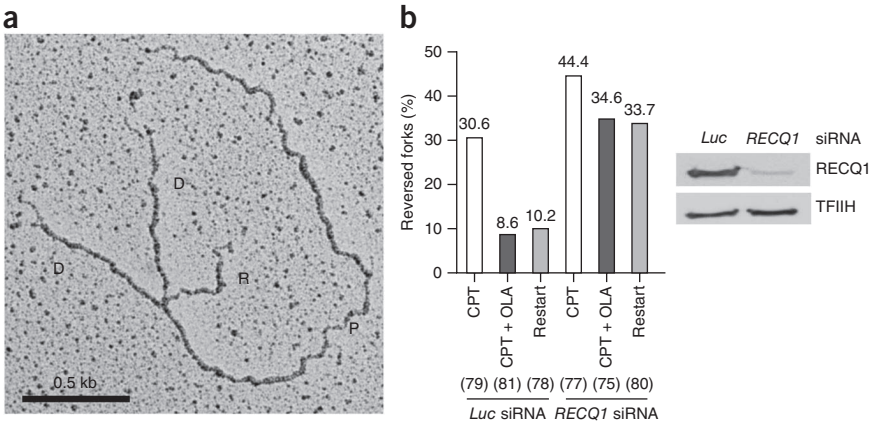

Figure 6 Reversed forks accumulate and are unable to restart in RECQ1-depleted cells after CPT treatment. (**a**) Representative electron micrograph of a reversed fork observed on genomic DNA from U-2 OS cells transfected with *RECQ1* siRNA and treated with CPT (25 nM) and olaparib (10 μM). D, daughter strand; P, parental strand; R, reversed arm. (**b**) Frequency of fork reversal in U-2 OS cells transfected with *Luc* siRNA or *RECQ1* siRNA and treated with CPT and/or olaparib. Restart experiments measuring the frequency of fork reversal were performed 3 h after CPT removal. Numbers above bars indicate proportion of reversed forks as a percentage of total number of molecules (bottom, parentheses). Right, RECQ1 expression after siRNA knockdown detected by western blotting. TFIIH, loading control.

the notion that RECQ1 depletion prevents DSB formation after PARP inhibition. Collectively, these data indicate that RECQ1 regulates the rate of replication fork progression and that RECQ1 depletion makes PARP activity dispensable in the prevention of DSB accumulation after TOP1 inhibition.

RECQ1 is essential for fork restart upon TOP1 inhibition

The observation that RECQ1 loss makes PARP activity dispensable in the prevention of fork slowing and DSB formation in CPT-treated cells suggests that regressed forks accumulate in RECQ1-depleted cells. This is in agreement with our biochemical results pointing to a role for RECQ1 in replication fork restart. To provide more direct evidence for this idea, we used EM to visualize the fine architecture of *in vivo* replication intermediates[31,32]. A previous EM analysis of replication intermediates showed that replication forks undergo rapid fork reversal upon TOP1 inhibition[7]. Furthermore, effective fork reversal required PARP1 activity, possibly by promoting the accumulation or stabilization of regressed replication forks and thus preventing fork collision with a CPT-induced lesion to generate a DSB[7]. To test the hypothesis that the accumulation of reversed forks is increased in RECQ1-depleted, CPT-treated cells, we used EM to compare RECQ1-depleted, CPT-treated U-2 OS cells in which PARP was inhibited to those in which it was not inhibited (**Fig. 6**). Consistent with previous findings, we observed a high frequency of fork reversal (approximately 30% of molecules analyzed) in control U-2 OS cells transfected with a small interfering RNA (siRNA) against *Luc* (encoding luciferase) and treated with 25 nM CPT. The same experiments performed in the presence of olaparib confirmed that PARP inhibition in control cells markedly decreased the fraction of reversed forks, from 30% to <10%. RECQ1 depletion by siRNA upon CPT treatment resulted in a higher frequency of fork reversal events (~44%) than that observed in control cells. Notably, PARP inactivation in RECQ1-depleted cells did not result in marked reduction in the fraction of regressed forks, suggesting that regressed forks do not restart upon RECQ1 inactivation, even in the absence of PARP activity. To test this hypothesis directly, we performed recovery experiments in which we measured reversed fork frequency after CPT removal. Whereas control cells showed a marked decrease in the frequency of fork reversal (from 30% to 10%) after drug removal, RECQ1-depleted cells maintained a high frequency of reversed forks (~33%) 3 h after CPT withdrawal. These data strongly suggest that RECQ1 is essential in restarting reversed forks and indicate that the requirement of PARP for CPT-induced fork reversal reflects a unique role for PARP in limiting RECQ1-mediated fork reactivation.

DISCUSSION

Replication fork regression is rapidly emerging as a pivotal response mechanism to the induction of replication stress. This notion is supported by the recent discovery that TOP1 inhibition by CPT induces replication fork slowing and reversal, preventing DSB formation at clinically relevant doses of CPT[7,8]. PARP1 is a crucial cellular mediator required for the accumulation or stabilization of regressed forks upon TOP1 poisoning. PARP1 itself is a target for anticancer therapies, particularly breast and ovarian cancers involving mutation of the genes *BRCA1* and *BRCA2*. PARP inactivation prevents the accumulation of regressed forks without affecting the checkpoint response[7]. However, the mechanism by which PARP activity promotes fork reversal is still unknown, and the requirements for the restart of reversed forks have not been defined. Our work provides new insight into these mechanisms by showing that regressed forks

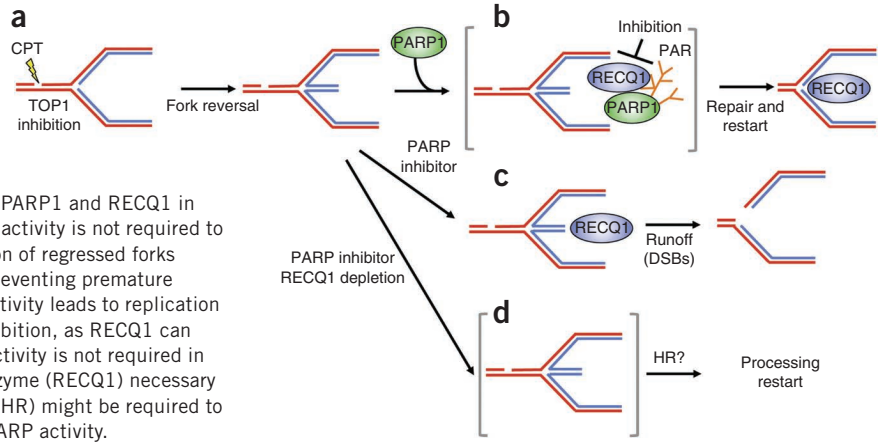

Figure 7 Schematic model of the combined roles of PARP1 and RECQ1 in response to TOP1 inhibition. (**a**,**b**) PARP PARylation activity is not required to form reversed forks, but it promotes the accumulation of regressed forks by inhibiting RECQ1 fork restoration activity, thus preventing premature restart of regressed forks. (**c**) Inhibition of PARP1 activity leads to replication runoff and increased DSB formation upon TOP1 inhibition, as RECQ1 can cause untimely restart of reversed forks. (**d**) PARP activity is not required in RECQ1-depleted cells because the cells lack the enzyme (RECQ1) necessary to promote fork restart. Homologous recombination (HR) might be required to promote fork restart in the absence of RECQ1 and PARP activity.

can restart *in vivo* and identifying a key role for human RECQ1 in promoting, through ATPase and branch migration activities, efficient replication fork restart after TOP1 inhibition (**Fig. 7**). Our results also show that this function of RECQ1 is not shared by other helicases, such as BLM and WRN. Furthermore, our results provide new insight into the molecular role of PARP in fork reversal by showing that the PARylation activity of PARP is important in regulating RECQ1 activity on replication forks after CPT treatment. A notable aspect of these data is that PARP activity is dispensable in the formation of reversed forks (**Fig. 7a**) but required to 'accumulate' them—that is, to maintain or protect them from counteracting activity (by RECQ1) that would otherwise cause an untimely restart of reversed forks, leading to DSB formation (**Fig. 7b**,**c**). Indeed, we show that in RECQ1-depleted cells, PARP activity is dispensable in the accumulation of reversed forks or the avoidance of CPT-induced DSBs (**Fig. 7d**). We propose that PARP 'signals' the presence of lesions on the template and inhibits RECQ1 locally, thereby restraining the restart of reversed forks until repair of the TOP1 cleavage complex is complete (**Fig. 7b**). An important next step will be to identify factors that modulate RECQ1-catalyzed fork restart by PARP activity.

These data provide a new mechanistic insight that could help to predict the efficiency of anticancer therapies that include both PARP and TOP1 inhibitors. These combinations are now in clinical trials. Our results also suggest that RECQ1 might represent a new therapeutic target to be used in conjunction with TOP1 inhibitors. In principle, induction of fork reversal (by TOP1 poisons) and inhibition of reversed fork reactivation (by RECQ1 depletion) should synergize, which would explain the observed CPT sensitivity of RECQ1-depleted cells.

RecQ helicases are DNA unwinding enzymes essential for the maintenance of genome stability in many organisms. Why human cells should express five RecQ homologs, and microorganisms such as *Escherichia coli*, *Saccharomyces cerevisiae* and *Schizosaccharomyces pombe* only one or two, remains unexplained. Our previous studies provided new insight by identifying important and distinct roles for RECQ1 and RECQ4 during DNA replication[19]. These data, combined with previous observations that RECQ1 depletion leads to increased DNA damage and affects cellular proliferation[27,33,34], suggest that RECQ1 might have a distinct role in the stabilization and repair of replication forks. Our discovery that RECQ1 is required for replication fork restoration after TOP1 poisoning provides what is, to our knowledge, the first indication of a specific cellular function for this RecQ helicase. U-2 OS cells lacking BLM or WRN do not show similar defects in replication fork restoration upon TOP1 poisoning, suggesting that RECQ1 is the RecQ helicase specifically responsible for promoting replication fork restart upon CPT-induced fork reversal. Moreover, RECQ1 shows a striking preference for fork restoration over regression, and its activity, unlike that of WRN, is specifically regulated by PARylation of PARP1 (ref. 26) (**Supplementary Fig. 7**). However, we cannot yet rule out the possibility that other human RecQ helicases are involved in different steps of the same process.

It will be important for future studies to determine whether reversed forks are detected in response to genotoxic stress other than TOP1 inhibition and whether RECQ1 or other helicases are implicated in replication fork reversal or restart, depending on the type of DNA damage. WRN- and BLM-deficient cells show increased sensitivity to select genotoxic agents[35], whereas RECQ1-deficient cells are markedly sensitive to CPT and etoposide, supporting the notion that these three RecQ helicases have distinct roles in replication stress response. The fact that RECQ1-depleted cells show increased sensitivity to etoposide opens the possibility that a similar mechanism of fork reversal and restart might take place upon treatment with topoisomerase II poisons. EM analysis of replication intermediates after treatment with different classes of chemotherapeutic drugs will provide early clues about combinations of drugs and RecQ helicases to pursue in future studies.

The discovery that RECQ1 is essential for fork restart upon TOP1 poisoning suggests that RECQ1 may itself be a new therapeutic target and that it could modulate the efficacy of combinatorial cancer therapies using PARP and TOP1 inhibitors that are already in clinical trials. A key experimental goal will be to determine the fate of regressed replication forks that accumulate in the absence of RECQ1. One possibility is that active replication forks are restored by the homologous-recombination machinery in the absence of the fork restart activity of RECQ1 (**Fig. 7d**). Thus, RECQ1 depletion or inhibition might result in synthetic lethality in a background deficient for homologous recombination, providing a new way to target and increase the efficacy of cancer therapies when homologous-recombination repair is inefficient or inhibited.

METHODS

Methods and any associated references are available in the online version of the paper.

Note: Supplementary information is available in the online version of the paper.

ACKNOWLEDGMENTS

We are grateful to A. Mazin for sharing information regarding the substrate preparation. We thank P. Janscak (University of Zurich) and D. Orren (University of Kentucky College of Medicine) for providing aliquots of purified WRN and WRN-E84A proteins, respectively. We thank G. de Murcia (École Supérieure de Biotechnologie de Strasbourg) for providing the constructs for the production of the PARP1 fragment. We thank Y. Ayala for critical discussions and G. Triolo for help in recombinant protein production. We thank the Nano Research Facility of the School of Engineering and Applied Science at Washington University in St. Louis, which is part of the National Nanotechnology Infrastructure Network supported by the US National Science Foundation under grant no. ECS-0335765, for microfabrication and the use of clean-room facility. We also thank the Center for Microscopy and Image Analysis of the University of Zurich for technical assistance with EM. This work was supported by startup funding from the Doisy Department of Biochemistry and Molecular Biology at the Saint Louis University School of Medicine and the Saint Louis University Cancer Center and grants from the President's Research Fund of Saint Louis University and the Associazione Italiana per la Ricerca sul Cancro (AIRC10510) to A.V.; US National Institutes of Health grant CA77852 to R.J.M. Jr.; Swiss National Science Foundation grants PP0033-114922 and PP00P3-135292 to M.L.; and a contribution from Fonds zur Förderung des Akademischen Nachwuchses (FAN) of the Zürcher Universitätsverein (ZUNIV) to M.L. and A.R.C.

AUTHOR CONTRIBUTIONS

M.B. conducted the immunoprecipitation, GST-pulldown, far-western and dot-blot experiments and the *in vitro* fork regression and restoration studies with the synthetic DNA substrates. A.R.C. conducted PFGE and EM analysis. S.T. conducted the single-molecule DNA replication assays. S. Gomathinayagam expressed the recombinant proteins and contributed to the *in vitro* fork regression and restoration assays. S.K. performed the immunofluorescence experiments and contributed to the cell-survival assays. M.V. conducted the single-molecule DNA replication assays with the BLM- and WRN-depleted cells. F.O. performed the protein complex purification experiments. T.G. contributed to the design of the proteomic experiments and performed MS analysis. S. Graziano performed the cell-survival assays. R.M.-M. contributed to the production of the GST-tagged fragments used in the GST-pulldown assays. F.M. contributed to the far-western analysis. B.L. produced the RECQ1 mutants and contributed to the optimization of protocols for RECQ1 expression. V.B. induced expression of the recombinant PARP1 protein. M.G. contributed to the design and supervision of the proteomic experiments. R.A. supervised the proteomic experiments. J.M.S. and R.J.M. Jr. contributed to the establishment of the single-molecule DNA replication assays in A.V.'s lab. R.J.M. Jr. assisted A.V. in finalizing the manuscript. M.L. planned, designed and supervised the PFGE and EM experiments and assisted A.V. in finalizing the manuscript. A.V. planned and supervised the project and wrote the manuscript.

COMPETING FINANCIAL INTERESTS
The authors declare no competing financial interests.

Published online at http://www.nature.com/doifinder/10.1038/nsmb.2501.
Reprints and permissions information is available online at http://www.nature.com/reprints/index.html.

1. Koster, D.A., Palle, K., Bot, E.S., Bjornsti, M.A. & Dekker, N.H. Antitumour drugs impede DNA uncoiling by topoisomerase I. *Nature* **448**, 213–217 (2007).
2. Pommier, Y., Leo, E., Zhang, H. & Marchand, C. DNA topoisomerases and their poisoning by anticancer and antibacterial drugs. *Chem. Biol.* **17**, 421–433 (2010).
3. Pommier, Y. Topoisomerase I inhibitors: camptothecins and beyond. *Nat. Rev. Cancer* **6**, 789–802 (2006).
4. Rodriguez-Galindo, C. *et al.* Clinical use of topoisomerase I inhibitors in anticancer treatment. *Med. Pediatr. Oncol.* **35**, 385–402 (2000).
5. Pommier, Y. *et al.* Repair of and checkpoint response to topoisomerase I–mediated DNA damage. *Mutat. Res.* **532**, 173–203 (2003).
6. Koster, D.A., Crut, A., Shuman, S., Bjornsti, M.A. & Dekker, N.H. Cellular strategies for regulating DNA supercoiling: a single-molecule perspective. *Cell* **142**, 519–530 (2010).
7. Ray Chaudhuri, A. *et al.* Topoisomerase I poisoning results in PARP-mediated replication fork reversal. *Nat. Struct. Mol. Biol.* **19**, 417–423 (2012).
8. Sugimura, K., Takebayashi, S., Taguchi, H., Takeda, S. & Okumura, K. PARP-1 ensures regulation of replication fork progression by homologous recombination on damaged DNA. *J. Cell Biol.* **183**, 1203–1212 (2008).
9. Bernstein, K.A., Gangloff, S. & Rothstein, R. The RecQ DNA helicases in DNA repair. *Annu. Rev. Genet.* **44**, 393–417 (2010).
10. Chu, W.K. & Hickson, I.D. RecQ helicases: multifunctional genome caretakers. *Nat. Rev. Cancer* **9**, 644–654 (2009).
11. Bachrati, C.Z. & Hickson, I.D. RecQ helicases: guardian angels of the DNA replication fork. *Chromosoma* **117**, 219–233 (2008).
12. Bohr, V.A. Rising from the RecQ-age: the role of human RecQ helicases in genome maintenance. *Trends Biochem. Sci.* **33**, 609–620 (2008).
13. Vindigni, A., Marino, F. & Gileadi, O. Probing the structural basis of RecQ helicase function. *Biophys. Chem.* **149**, 67–77 (2010).
14. Bugreev, D.V., Rossi, M.J. & Mazin, A.V. Cooperation of RAD51 and RAD54 in regression of a model replication fork. *Nucleic Acids Res.* **39**, 2153–2164 (2011).
15. Machwe, A., Karale, R., Xu, X., Liu, Y. & Orren, D.K. The Werner and Bloom syndrome proteins help resolve replication blockage by converting (regressed) Holliday junctions to functional replication forks. *Biochemistry* **50**, 6774–6788 (2011).
16. Machwe, A., Lozada, E., Wold, M.S., Li, G.M. & Orren, D.K. Molecular cooperation between the Werner syndrome protein and replication protein A in relation to replication fork blockage. *J. Biol. Chem.* **286**, 3497–3508 (2011).
17. Hickson, I.D. RecQ helicases: caretakers of the genome. *Nat. Rev. Cancer* **3**, 169–178 (2003).
18. Seki, M. *et al.* Purification of two DNA-dependent adenosinetriphosphatases having DNA helicase activity from HeLa cells and comparison of the properties of the two enzymes. *J. Biochem.* **115**, 523–531 (1994).
19. Thangavel, S. *et al.* Human RECQ1 and RECQ4 helicases play distinct roles in DNA replication initiation. *Mol. Cell Biol.* **30**, 1382–1396 (2010).
20. Glatter, T., Wepf, A., Aebersold, R. & Gstaiger, M. An integrated workflow for charting the human interaction proteome: insights into the PP2A system. *Mol. Syst. Biol.* **5**, 237 (2009).
21. Ying, S., Hamdy, F.C. & Helleday, T. Mre11-dependent degradation of stalled DNA replication forks is prevented by BRCA2 and PARP1. *Cancer Res.* **72**, 2814–2821 (2012).
22. Sharma, S., Phatak, P., Stortchevoi, A., Jasin, M. & Larocque, J.R. RECQ1 plays a distinct role in cellular response to oxidative DNA damage. *DNA Repair (Amst.)* **11**, 537–549 (2012).
23. Wang, Y., Li, H., Tang, Q., Maul, G.G. & Yuan, Y. Kaposi's sarcoma-associated herpesvirus ori-Lyt-dependent DNA replication: involvement of host cellular factors. *J. Virol.* **82**, 2867–2882 (2008).
24. Kleine, H. & Luscher, B. Learning how to read ADP-ribosylation. *Cell* **139**, 17–19 (2009).
25. Schreiber, V. *et al.* Poly(ADP-ribose) polymerase-2 (PARP-2) is required for efficient base excision DNA repair in association with PARP-1 and XRCC1. *J. Biol. Chem.* **277**, 23028–23036 (2002).
26. von Kobbe, C. *et al.* Poly(ADP-ribose) polymerase 1 regulates both the exonuclease and helicase activities of the Werner syndrome protein. *Nucleic Acids Res.* **32**, 4003–4014 (2004).
27. Sharma, S. & Brosh, R.M. Jr. Human RECQ1 is a DNA damage responsive protein required for genotoxic stress resistance and suppression of sister chromatid exchanges. *PLoS ONE* **2**, e1297 (2007).
28. Bugreev, D.V., Mazina, O.M. & Mazin, A.V. Rad54 protein promotes branch migration of Holliday junctions. *Nature* **442**, 590–593 (2006).
29. Ferro, A.M. & Olivera, B.M. Poly(ADP-ribosylation) *in vitro*. Reaction parameters and enzyme mechanism. *J. Biol. Chem.* **257**, 7808–7813 (1982).
30. Hanada, K. *et al.* The structure-specific endonuclease Mus81 contributes to replication restart by generating double-strand DNA breaks. *Nat. Struct. Mol. Biol.* **14**, 1096–1104 (2007).
31. Lopes, M. Electron microscopy methods for studying *in vivo* DNA replication intermediates. *Methods Mol. Biol.* **521**, 605–631 (2009).
32. Neelsen, K.J., Ray Chaudhuri, A., Follonier, C., Herrador, R. & Lopes, M. Visualization and interpretation of eukaryotic DNA replication intermediates by electron microscopy *in vivo*. *Methods Mol. Biol.* (in the press).
33. Mendoza-Maldonado, R. *et al.* The human RECQ1 helicase is highly expressed in glioblastoma and plays an important role in tumor cell proliferation. *Mol. Cancer* **10**, 83 (2011).
34. Sharma, S. *et al.* RECQL, a member of the RecQ family of DNA helicases, suppresses chromosomal instability. *Mol. Cell Biol.* **27**, 1784–1794 (2007).
35. Mao, F.J., Sidorova, J.M., Lauper, J.M., Emond, M.J. & Monnat, R.J. The human WRN and BLM RecQ helicases differentially regulate cell proliferation and survival after chemotherapeutic DNA damage. *Cancer Res.* **70**, 6548–6555 (2010).
36. Langelier, M.F., Servent, K.M., Rogers, E.E. & Pascal, J.M. A third zinc-binding domain of human poly(ADP-ribose) polymerase-1 coordinates DNA-dependent enzyme activation. *J. Biol. Chem.* **283**, 4105–4114 (2008).
37. Tao, Z., Gao, P., Hoffman, D.W. & Liu, H.W. Domain C of human poly(ADP-ribose) polymerase-1 is important for enzyme activity and contains a novel zinc-ribbon motif. *Biochemistry* **47**, 5804–5813 (2008).

ONLINE METHODS

Materials. The antibodies used were rabbit polyclonal antibody to PARP1 (anti-PARP1) Enzo, ALX-210-302-R100) (1:2,000), mouse monoclonal anti-PARP1 (Santa Cruz, sc-8007) (1:1,000), mouse monoclonal anti-PAR (Enzo, ALX-804-220-R100, clone 10H) (1:2,000), rabbit polyclonal anti-PAR (Trevigen, 4336-BPC-100) (1:2,000), mouse monoclonal anti-Ku70 and anti-Ku86 (Santa Cruz, sc-5309 and sc-5280) (1:2,000), mouse monoclonal anti-tubulin (Sigma, T5168) (1:5,000), mouse monoclonal anti-WRN (BD laboratories, 611169) (1:1,000), rabbit polyclonal anti-BLM (Abcam, ab476) (1:1,000), rabbit polyclonal anti-TFIIH (Santa Cruz, sc293) (1:2,000), rabbit polyclonal anti-RECQ1 raised against residues 1–110 (Santa Cruz, sc-25547) (1:2,000) and a custom-made rabbit anti-RECQ1 polyclonal antibody to a synthetic peptide of a unique sequence in the last 16 residues at the C terminus of RECQ1 (Sigma) (1:2,000)[33]. Camptothecin and etoposide were from Sigma. The PARP1 inhibitors olaparib and NU1025 were from Selleck Chemicals and Sigma, respectively.

Protein complex purification. To isolate protein complexes containing a RECQ1 bait protein, we prepared a HEK293 cell line expressing a double-tagged version of the human RECQ1 helicase by Flp recombinase-mediated integration. This system allows the generation of stable mammalian cell lines exhibiting tetracycline-inducible expression of a gene of interest from a single genomic location[20]. The protein complexes containing RECQ1 were isolated and analyzed by MS as previously described[20] (**Supplementary Fig. 1**).

Immunoprecipitation. HEK293T or human osteosarcoma U-2 OS cells were treated as indicated, washed two times with ice-cold PBS and resuspended in cytoplasmic extraction buffer (10 mM Tris-HCl (pH 7.9), 0.34 M sucrose, 3 mM CaCl2, 2 mM magnesium acetate, 0.1 mM EDTA, 1 mM DTT, 20 mM NaF, 10 mM β-glycerophosphate, 0.2 mM Na_3VO_4, 0.5% Nonidet P-40 and protease inhibitors (Roche)) for 10 min at 4 °C. Intact nuclei were pelleted by low-speed centrifugation, washed with cytoplasmic lysis buffer (without Nonidet P-40) and lysed in nuclear lysis buffer (20 mM HEPES (pH 7.9), 150 mM KCl, 1.5 mM $MgCl_2$, 20 mM NaF, 10 mM β-glycerophosphate, 0.2 mM Na_3VO_4 10% glycerol, 0.5% Nonidet P-40 and protease inhibitors) by homogenization, and DNA and RNA in the suspension were digested with 50 U per microliter Benzonase (Sigma) at 4 °C for 1 h. The nuclear-soluble extract was clarified from insoluble material by centrifugation at 20,000 × *g* for 20 min, pre-cleared with a 50-µl slurry of protein A beads (Santa Cruz) at 4 °C for 1 h and incubated overnight with anti-RECQ1 (Sigma), anti-PARP1 (Enzo) or a control IgG rabbit polyclonal antibody at 4 °C. Immunocomplexes were captured by adding 50 µl of a protein A bead slurry for 2 h at 4 °C. After extensive washing, proteins were eluted from beads with 2× Laemmli sample buffer at 95 °C for 5 min, separated by SDS-PAGE and detected by immunoblotting with the appropriate antibodies.

GST pulldown experiments with *in vitro*–translated PARP1. Pulldown assays with GST-RECQ1 fragments were performed as previously described[38]. Briefly, [^{35}S]Met-labeled, *in vitro*–translated PARP1 was incubated with GST-fused RECQ1 fragments bound to 10 µl of glutathione-Sepharose beads (Amersham) in binding buffer TNEN (20 mM Tris-HCl (pH 7.5), 150 mM NaCl, 1.0 mM EDTA (pH 8.0), 0.5% NP-40, 1 mM DTT and 1 mM PMSF) supplemented with 0.1 mg/ml ethidium bromide for 2 hr at 4 °C. The beads were subsequently washed two times in ethidium bromide–supplemented TNEN buffer and three times with TNEN buffer. Bound proteins were eluted with SDS sample buffer, resolved by gel electrophoresis and visualized by autoradiography. For the pulldowns with the GST-PARP1 fragments, [^{35}S]Met-labeled, *in vitro*-translated RECQ1 was incubated with immobilized GST or GST–PARP1 domains. The GST-PARP fragments were expressed in HeLa cells as previously described[25,26]. Cells were lysed 48 h later in 50 mM Tris-HCl (pH 8), 250 mM NaCl, 0.5% NP-40, 0.5 mM PMSF and protease inhibitors. Lysates were cleared by centrifugation and incubated for 2 h with glutathione-Sepharose beads. Beads were washed three times with lysis buffer and two times with lysis buffer supplemented with 1 M NaCl and resuspended in GST binding buffer for pulldown experiments with the purified GST-PARP1 fragments.

PAR binding assay. The PAR binding assays were performed using 1 M NaCl for the washing step as previously described[39].

Purification of recombinant proteins and *in vitro* PARylation of PARP1. Recombinant RECQ1 and PARP1 were purified from insect cells as previously described[40,41]. For *in vitro* poly(ADP-ribosyl)ation of PARP1, recombinant PARP-1 was incubated in 20 µl of activity buffer (50 mM Tris (pH 7.5), 4 mM $MgCl_2$, 50 mM NaCl, 200 µM DTT, 0.1 µg/µl BSA, 4 ng/µl DNaseI-activated calf thymus DNA and 400 µM NAD^+) for 10 min at 37 °C.

***In vitro* fork regression and restart assays.** The oligonucleotide sequences and the procedure used for the preparation of [γ-^{32}P]ATP-labeled substrate are shown in **Supplementary Table 1** and **Supplementary Figure 3**, respectively. Reactions were performed using the indicated protein concentrations and 2 nM DNA substrate in branch migration buffer (35 mM Tris-HCl (pH 7.5), 20 mM KCl, 5 mM $MgCl_2$, 0.1 mg/ml BSA, 2 mM DTT, 15 mM phosphocreatine, 30 U/ml creatine phosphokinase and 5% glycerol) at 37 °C. The reaction was started by the addition of 2 mM ATP. Concentration-dependence experiments were stopped after 20 min. For the poly(ADP-ribosyl)ation experiments, the indicated concentrations of PARP1 and 200 µM NAD or 100 nM purified PAR were added to the reaction mixture without ATP and pre-incubated together with RECQ1 and the substrate at 37 °C for 10 min. DNA substrates were deproteinized by adding 3× stop reaction (1.2% SDS, 30% glycerol supplemented with proteinase K (3mg/ml)) at room temperature for 10 min before being resolved on a native 8% polyacrylamide gel run in Tris-borate-EDTA (TBE) buffer at 4 °C.

Genetic knockdown–rescue assays. siRNA-mediated transient depletion of RECQ1 was achieved using an siRNA SMART pool against human *RECQ1* (NM_032941, Dharmacon) in U-2 OS cells and a previously described protocol in which we established the specificity of the siRNA pool[19,33]. siRNA-mediated depletion of WRN and BLM was achieved using the following siRNAs from Microsynth: *WRN* siRNA (5′-UAGAGGGAAACUUGGCAAAdTdT-3′) and *BLM* siRNA (5′-CCGAAUCUCAAUGUACAUAGA dTdT-3′). shRNA-mediated downregulation was achieved by cloning the sequence targeting *RECQ1* (5′-GAGCTTATGTTACCAGTTA-3′) into the pLKO.1 lentiviral shRNA expression vector. Virus was generated by transient cotransfection of pLKO.1 and the packaging plasmids psPAX2 and pM2D.G into 293T cells. Viral supernatants were filtered through a 0.45 µM filter and transduced on U-2 OS cells for 24 h, followed by selection with puromycin (8 µg/ml) for 3 d. Control transductions were performed using the pLKO.1 vector expressing a shRNA targeting the gene encoding Luciferase (5′-ACGCTGAGTACTTCGAAATGT-3′). The level of depletion was verified by western blotting. For the complementation assays, we cloned a *RECQ1* RNAi–resistant open reading frame into a pIRES vector under the control of the CMV promoter. Specifically, the nucleotides targeted by the RNAi (5′-GAGCTTATGTTACCAGTTA-3′) were partially substituted without changing the amino acid sequence (5′-GTCACTATGCTATCAATTA-3′) by site-directed mutagenesis. Lentiviral depletion of endogenous RECQ1 was achieved using the protocol described above, and the resulting RECQ1-depleted cells were then nucleofected with a shRNA-resistant RECQ1 expression vector. Expression of the RNAi-resistant, Flag-tagged RECQ1 and K119R mutant was verified in control and RECQ1-depleted cells by western analysis 48 h after transfection.

Microfluidic-assisted DNA fiber stretching and replication fork progression analysis. Asynchronous U-2 OS cells were transiently transfected for 72 h with siRNA SMART pools (or specific shRNA) against RECQ1 or Luciferase as reported earlier[19,33]. RECQ1- or Luciferase-depleted U-2 OS cells were labeled for 30 min each with 50 µM CldU followed by 50 µM IdU. Cells were collected by trypsinization, and high–molecular weight DNA from cells embedded in agarose plugs was isolated and stretched using a microfluidic platform as described earlier[42]. For immunostaining, stretched DNA fibers were denatured with 2.5 N HCl for 45 min, neutralized in 0.1 M sodium borate (pH 8.0) and PBS, and blocked with PBS, 5% BSA and 0.5% Tween-20 for 30 min. Rat anti-CldU/BrdU (Abcam, ab6326) (1:6), goat anti-rat Alexa 594 (Invitrogen, A11007) (1:1,000), mouse anti-IdU/BrdU (BD Biosciences, 347580) (1:6) and goat anti-mouse Alexa 488 (Invitrogen, A11001) (1:1,000) antibodies were used to reveal CldU- and IdU-labeled tracts, respectively. A Leica SP5X confocal microscope was used to visualize the labeled tracts, and tract lengths were measured using ImageJ (http://rsbweb.nih.gov/ij/). Statistical analysis of the tract length was performed using GraphPad Prism (http://www.graphpad.com/scientific-software/prism/).

Double-strand break detection by pulsed-field gel electrophoresis. DSB detection by PFGE was performed as previously described with minor modifications[7,30].

Immunofluorescence analyses. U-2 OS cells were grown on coverslips, fixed in 3.7% PFA, permeabilized in 0.5% Triton X-100 and blocked in 3% BSA. Coverslips were then stained with rabbit polyclonal anti-53BP1 (Novus Biologicals, NB100-304) (1:500) and mouse monoclonal anti-γH2AX (Millipore, 05-636) (1:300), and detected by appropriate Alexa 488– and Alexa 594–conjugated secondary antibodies (1:700). Toto3 iodide (Life Technologies, T3604) was used as a nuclear counter-stain. Cells were imaged using a Zeiss LSM 510 Meta confocal microscope. Images were acquired using the LSM 5 software. Foci were counted with ImageJ 'Analyze particles' function and 'JACoP' plugin was used to calculate colocalization. The average number of foci was obtained from three independent experiments analyzing at least 35 cells per sample.

Electron microscopy analysis of genomic DNA in mammalian cells. EM analysis of replication intermediates has been described in detail[31,32], including a description of the important parameters to consider specifically for the identification and the scoring of reversed forks[32].

38. Lucic, B. *et al.* A prominent β-hairpin structure in the winged-helix domain of RECQ1 is required for DNA unwinding and oligomer formation. *Nucleic Acids Res.* **39**, 1703–1717 (2011).
39. Ahel, D. *et al.* Poly(ADP-ribose)-dependent regulation of DNA repair by the chromatin remodeling enzyme ALC1. *Science* **325**, 1240–1243 (2009).
40. Cui, S. *et al.* Analysis of the unwinding activity of the dimeric RECQ1 helicase in the presence of human replication protein A. *Nucleic Acids Res.* **32**, 2158–2170 (2004).
41. Muzzolini, L. *et al.* Different quaternary structures of human RECQ1 are associated with its dual enzymatic activity. *PLoS Biol.* **5**, e20 (2007).
42. Sidorova, J.M., Li, N., Schwartz, D.C., Folch, A. & Monnat, R.J. Jr. Microfluidic-assisted analysis of replicating DNA molecules. *Nat. Protoc.* **4**, 849–861 (2009).

doi:10.1038/nsmb.2501